



Original research article

Computational formulation and immune dynamics of a multi-peptide vaccine candidate against Crimean-Congo hemorrhagic fever virus



Md. Shakil Ahmed Khan^a, Zulkar Nain^a, Shifath Bin Syed^a, Faruq Abdulla^b, Mohammad Ali Moni^c, Md. Moinuddin Sheam^a, Mohammad Minnatul Karim^{a, **}, Utpal Kumar Adhikari^{d, *}

^a Department of Biotechnology and Genetic Engineering, Faculty of Biological Sciences, Islamic University, Kushtia, 7003, Bangladesh

^b Department of Statistics, Faculty of Sciences, Islamic University, Kushtia, 7003, Bangladesh

^c WHO Collaborating Centre on eHealth, UNSW Digital Health, School of Public Health and Community Medicine, Faculty of Medicine, UNSW, Sydney, Australia

^d School of Medicine, Western Sydney University, Campbelltown, NSW, 2560, Australia

ARTICLE INFO

Keywords:

Crimean-Congo hemorrhagic fever
Immunoinformatics
Multipeptope vaccine
Molecular docking

ABSTRACT

The sole objective of this research is to devise an epitope-based vaccine candidate as prophylaxis for the Crimean-Congo hemorrhagic fever virus (CCHFV) using the knowledge of immunoinformatics and structural biology. Importantly, CCHFV outbreaks have increased in several countries resulting in increased mortality up to 40% due to the lack of prospective medication and an efficient vaccine. In this study, we have used several immunoinformatic tools and servers to anticipate potent B-cell and T-cell epitopes from the CCHFV glycoprotein with the highest antigenicity. After a comprehensive evaluation, a vaccine candidate was designed using 6 CD8⁺, 3 CD4⁺, and 7 B-cell epitopes with appropriate linkers. To enhance the vaccine's efficiency, we added *Mycobacterium tuberculosis* lipoprotein LprG (Rv1411c) to the vaccine as an adjuvant. The final construct was composed of a total of 468 amino acid residues. The epitope included in the construct showed 98% worldwide population coverage. Importantly, the construct appeared as antigenic, immunogenic, soluble, and non-allergenic in nature. To explore further, we modelled the three-dimensional (3D) structure of the constructed vaccine. Our chimeric vaccine showed stable and strong interactions for toll-like receptor 2 (TLR2) found on the cell surface. Moreover, the dynamics simulation of immune response showed elevated levels of cellular immune activity and faster clearance of antigen from the body upon repetitive exposure. Finally, the optimized codon (CAI≈1) ensured the marked translation efficiency of the vaccine protein in *E. coli* strain K12 bacterium followed by the insertion of construct DNA into the cloning vector pET28a (+). We believe that the designed vaccine chimera could be useful in vaccine development to fight CCHFV outbreaks.

1. Introduction

Crimean-Congo hemorrhagic fever virus (CCHFV) is a tick-borne infectious ssRNA virus under the *Nairovirus* genus and caused several outbreaks of viral hemorrhagic fever [1]. In 1940, the CCHFV was first identified in the Crimean Peninsula and now spread over 30 countries. In particular, countries/regions in Asia, Europe, Africa, and the Middle-East are prone to this viral infection [2]. Recently, several CCHFV outbreaks have occurred in south-western Russia, Central Africa, and Spain [3]. Besides, a number of cases were reported in Albania, Turkey, and Georgia from 2001 to 2009 [4]. The viral transmission

through infected patient and cattle viremia, along with the ecological complexity and therapeutic controversy, is the primary reason for viral outbreaks [5]. The mortality risk of CCHFV infection is up to 40% [6].

The RNA genome of CCHFV encodes three major proteins, i.e., nucleocapsid (N), glycoprotein (GP), and RNA-dependent RNA polymerase (RdRP) [7]. Among the viral proteins, viral GP plays a major role in pathogenesis, especially in the interaction with vertebrate and tick hosts, as well as in cell tropism [8]. It is also involved in CCHFV immune response [9]. The major symptoms include high fever, headache, myalgia, diarrhea, and hypotension that eventually lead to epistaxis, ecchymosis, bleeding gums, and emesis [6]. The remedy broadly lies in

* Corresponding author.

** Corresponding author.

E-mail addresses: mmk@btge.iu.ac.bd (M.M. Karim), u.adhikari@westernsydney.edu.au (U.K. Adhikari).

complication management [10]. Recently, a drug called ribavirin has been suggested as a therapeutic medication. However, ribavirin's efficacy is found controversial, especially in delayed phase of CCHFV infection [11,12]. In addition, immunoglobulin-based therapy by antibody engineering still remains in its infancy [13]. Moreover, several vaccine trials against CCHFV have been terminated for their high toxicity [13]. The difficulties in manufacturing live or inactivated vaccines lie in the genetic variability in CCHFV serotypes [6]. Notably, several attempts have been made to generate a functional CCHFV vaccine in recent years. For instance, Garrison et al. developed and tested a DNA vaccine on mice models [14]. Although it was able to elicit immune responses in two of the mouse models, the exact protective mechanism remains uncertain. Besides, its ability to provoke cross-protective immunity to other CCHFV strains is unknown [14]. Furthermore, transcriptionally-competent virus-like particles (tc-VLPs) have been used against CCHFV [15]. Despite the production of robust neutralizing antibody titers, the tc-VLPs showed a protective effect on only 40% of animals [16]. Moreover, several other vaccine candidates were failed to show either protection or safety to hosts [17,18]. Therefore, there are no licensed vaccines or medications available at present to fight against CCHFV infection.

In recent years, computational immunology has been used to design a multiepitope vaccine that is devoid of toxic, allergic, or other unwanted peptide fragments. A number of multiepitope vaccines against viruses, bacteria, and parasites have been designed using the immunoinformatics approach [19–25]. The principal focus on these studies is to highlight the potential immunodominant epitopes among the bulk of epitopes from the certain pathogens that can be used to which are evaluated for their immunogenic properties as a vaccine candidate. To overcome the early problem in developing vaccination against CCHFV, epitope-based peptide vaccine could be a good strategy since it can be designed with specific and desired characteristics [26]. Identification of potential epitopes in CCHFV proteins along with candidate vaccine design using immunoinformatics has also been done previously [1]. However, those studies were limited to a single protein, thus, lack of specificity towards a wide range of genetically different CCHFV strains [1,27]. Moreover, lack of immune simulation has failed to show the probable immune reactions triggered against the CCHFV, which is very important while assessing vaccine candidates.

Therefore, we aimed to design a multiepitope vaccine against CCHFV by employing a series of computational biology techniques followed by standard docking, molecular dynamics, and immune simulation studies. In this case, we considered viral GP as the epitope source and both T-cells and B-cells for vaccine design to provoke both antibody and cell-mediated immune activities. For structural improvement, we engineered the vaccine to facilitate disulfide bridging while codons were optimized and *in silico* cloning were performed for efficient translation.

2. Methodology

2.1. Retrieval of protein sequence

At the very beginning, we retrieved the protein sequences of CCHFV in FASTA format from the ViPR (Virus Pathogen Database and Analysis Resource) database [28]. For individual virus families and species, ViPR is an enrich database consolidated with the NCBI (National Centre for Biotechnology Information) as well as the UniProtKB database; and also supported by the NIAID (National Institute of Allergy and Infectious Diseases). After analyzing, we categorized different types of proteins as glycoprotein (GP), glycoprotein precursor (GP precursor), L-protein, envelope glycoprotein (EGP), envelope glycoprotein precursor (EGP precursor), membrane glycoprotein (Membrane GP), N-protein, nucleocapsid protein, nucleoprotein, polymerase, pre-glycoprotein (Pre-GP), and transcriptase.

2.2. Highest antigenic protein prediction

Antigenicity implies the ability to initiate an immune reaction against the antigen. All CCHFV protein sequences were evaluated in VaxiJen v2.0 server with 0.5 thresholds [29]. The ACC (auto cross-covariance) transformation process helps the server to sustain 70–89% accuracy in prediction. The antigenicity prediction developed based on the physicochemical properties, not on the sequence alignment of proteins [30]. Antigenicity was demonstrated by GP, GP precursor, membrane GP, pre-GP, EGP, and EGP precursor. For further study, protein with the highest antigenicity has been chosen.

2.3. CD8⁺ epitopes and MHC class I alleles prediction

The NetCTL v1.2 server was employed to determine the CD8⁺ epitopes for twelve (12) supertypes available in the server [31]. This web-tool anticipates all possible epitopes by combining the estimation of proteasomal cleavage and TAP transport efficiency as well as the MHC class I affinity. For this purpose, artificial neural network (ANN) is applied for MHC-I allele and C-term cleavage, while Weight-Matrix is to evaluate the TAP transporting efficiency [31]. The cutoff score was set to 0.5 with the sensitivity of 0.89 and specificity of 0.94. Furthermore, IEDB analysis tool was implemented to predict MHC-I binding alleles with a consensus method [32]. The predicted alleles were analyzed with ≤ 5 percentile rank since the lower score indicates higher affinity. Vaccine development relies on immunogenicity. Hence, the immunogenicity of the epitopes should be screened [33]. The IEDB Immunogenicity tool was utilized to presume the immunogenicity of CD8⁺ epitopes [34]. The antigenic properties of those epitopes were also evaluated through the VaxiJen v2.0 server to ensure their ability to trigger specific immune reactions [30]. The AllergenFP v1.0 web-tool estimated the allergenicity of the CD8⁺ epitopes. This server predicts probable allergen with 89% accuracy based on the physicochemical properties and secondary structure-forming propensities of the input epitope [35]. Furthermore, the epitopes were screen for toxic nature with the ToxinPred server based on quantitative-matrix (QM) and machine-learning (ML) techniques [36].

2.4. CD4⁺ epitopes and MHC class II alleles prediction

We predicted CD4⁺ epitopes with respective MHC-II alleles using the MHC-II binding tool present in IEDB database. To do so, NN-align method was applied, which performs better than both the SMM-align and NetMHCIIpan methods [37]. CD4⁺ cells are very crucial in vaccine development, and activates the interleukin-4 (IL-4), interferon-gamma (IFN- γ), and interleukin-10 (IL-10) cytokines [38]. Therefore, the IFNepitope web-tool was used to identify IFN- γ positive CD4⁺ epitopes applying hybrid method (both motif and SVM techniques) that provides 81.39% of accurate prediction [39]. Contrastingly, IL-4 and IL-10 generating CD4⁺ epitopes were determined by IL4pred (with 75.76% accuracy) and IL10pred (with 81.24% accuracy) servers, respectively, by maintaining default parameters [39,40].

2.5. Linear B-cell (LBC) epitopes prediction

B-lymphocyte plays a fundamental role in our humoral immunity by generating immunoglobulins upon interacting to the antigens [41]. Hence, the presence of B-cell epitopes is essential for vaccine construction. However, there are two forms of B-cell epitopes - linear and conformational. For vaccine construction, we considered linear B-cell (LBC) epitopes. The LBtope web-server was applied to anticipate the LBC epitopes based on the three different algorithms - protein shape estimation, residue's protrusion scale and neighbor clustering [42]. In addition, extensive assessment was conducted with VaxiJen v2.0, AllergenFP v1.0, and ToxinPred web-tools for the selection of

appropriate LBC epitopes in terms of antigenicity, allergenicity, and toxicity, respectively.

2.6. Global population coverage index

The spread and features of HLA-alleles differ based on the regions and ethnicity around the globe. In addition, the binding efficacy of CD8⁺ and CD4⁺ epitopes differ from allele to allele. To evaluate the allele coverage by the selected epitopes, we used the IEDB tool of population coverage [43]. It was schemed to calculate the population coverage according to various countries, regions, and ethnicities around the world.

2.7. Designing of multiepitope vaccine construct

A multiepitope vaccine map was constructed using the potent CD8⁺, CD4⁺, and LBC epitopes with appropriate adjuvant & linkers, as described earlier [19]. In doing so, CD8⁺ epitopes were linked together with AAY linker, while CD4⁺ epitopes were added using GPGPG linker. Further, KK linkers were employed to fuse LBC epitopes. To increase the vaccine's immunogenicity, we also added mycobacterial lipoprotein LprG (Genbank ID: 886,700) as adjuvant ahead of the first epitope with EAAAK linker. This lipoprotein is a prominent toll-like receptor 2 (TLR2) agonist.

2.8. Physicochemical and immunological evaluation

Immunogenicity means the ability of our immune system to protect the host from invading pathogens, abnormal self-antigens by stimulating antibody and cell-mediated immune reactivities, while the antigenic recognition ability of the immune system is called antigenicity. Hence, their definition proved that all immunogens are known to be antigens. However, all antigens are not immunogens [44]. The constructed vaccine was evaluated with the VaxiJen v2.0 web-server to identify the antigenic feature of the candidate vaccine. AllergenFP v1.0 web-tool was applied to check the allergenicity. We used the ProtParam server to check the physicochemical characteristics of the construct i.e., molecular weight (MW), theoretical isoelectric point (pI), instability index (II), *in vitro* and *in vivo* half-life, aliphatic index (AI), and grand average of hydropathicity (GRAVY) [45]. Furthermore, the SOLpro tool was used to predict the solubility of recombinant chimeric vaccine on over-expression in *E. coli*, as a prerequisite for structural, functional, and biochemical studies [46].

2.9. Homology modelling, refinement, and validation

The three-dimensional (3D) structure of the chimera was modelled by I-TASSER server. It uses multiple-template threading to determine the best template based on which the protein will be built by assembling iterative template fragments and provides a confidence (C) score for each predicted 3D model [47]. The crude model of the 3D vaccine model was fine-tuned with GalaxyRefine webserver. This server repacks side-chain, re-builds unreliable loops, and relaxes the structure by applying dynamics simulation [48]. To check if the structure refined, we submitted the refined vaccine's structure to ProSA-web server [49] and RAMPAGE web-server [50] for validation purposes. The ProSA-web evaluates the protein structure by comparing it with the NMR and X-ray crystallography derived validated structures and provided a score as an overall quality factor. RAMPAGE server creates a Ramachandran plot and provides the number of energetically favored, allowed, and disallowed residues.

2.10. Study of molecular docking simulation

The molecular docking is a computer-based analytical method for binding affinity and interaction between the receptor and ligand. It was

reported that TLR2 sensed the negative-sense ssRNA viruses [51]. Besides, TLR2 heterodimers initiate the cytokine signaling that activates CD8⁺ cells to identify viral antigens and help to reduce virus loads [52]. Therefore, we considered TLR2 as the receptor while vaccine protein as the ligand. The TLR2 molecule (PDB ID: 3A7C) was obtained from the RCSB PDB server [53]. The binding affinity and interaction between the vaccine and TLR2 receptor were finally anticipated with the ClusPro web-based docking server [54]. This server executed the docking in three steps: (1) rigid-body docking, (2) clustering of structure with minimal energy, and (3) structural refinement [54]. Based on the energy score, the best-docked complex with suitable pose was determined.

2.11. In silico codon optimization and cloning

The codon adaptation is the process to optimize the codon present in a foreign gene according to the codon present in the host gene for quality gene expression [19]. We used Java Codon Adaptation Tool (JCat) to optimize our vaccine's codon according to the widely used *E. coli* strain K12 [55]. From the JCat server, three additional options, i.e., rho-independent termination of transcription process, ribosome binding sites in prokaryotes, and restriction cleavage sites were avoided since they are conserved in the prokaryotic systems [56]. Additionally, the N and C terminal were incorporated with the *Xba*I and *Nde*I restriction sites of the modified DNA sequence, respectively. Finally, we inserted the adapted DNA into *E. coli* pET28a (+) vector for cloning the vaccine with SnapGene v4.2 tool.

2.12. Simulation of immune reactions

To check the vaccine's efficiency in triggering an immune response, we used an immune simulator available in the C-ImmSim server as described earlier [20,57]. C-ImmSim server applies a PSSM (position-specific scoring matrix) and ML techniques for agent-based dynamics simulation to predict epitopes and respective immune reactions [57]. In general, most vaccines are given in three doses with 28 days interval. Therefore, we decided to administer three injections (doses) in which an interval between two doses was 4 weeks. Each time-step in C-ImmSim immune simulator is defined to be equivalent to 8 h in real life; hence, required 1, 84, and 168 timesteps for three injections. Furthermore, antigen exposure in a typical endemic zone was evaluated using a total of 6 injections as repeated exposure.

2.13. Molecular dynamics simulation

To determine the structural stability and integrity of the docked complex, we simulated the molecular dynamics (MD). The software-based simulation of MD was performed utilizing YASARA Dynamics under the AMBER14 force-field [58,59] while iMODS server [60] was used for server-based MD simulation. For software-based MD simulation, the complex was engineered for the addition of hydrogen in the whole complex to form a simulation-cell filled with water (model: TIP3P; density: 0.997 g/L-1). Cut-off radius for short-range interactions in physiologic states (temperature: 298 K, pH range: 7.4; salt: 0.9% NaCl) was set to 8.0 Å. The simulation was executed for 5 ns with a time-step of 1.25 fs and snapshots were captured at every 100 ps (ps). Finally, these trajectories were analyzed to calculate the RMSD (root mean square deviation), RMSF (root mean square fluctuation), and radius of gyration (Rg), respectively. For server-based MD studies, the complex was submitted to the iMODS server. Based on the NMA (normal mode analysis) method, it provides deformability, Eigenvalues, B-factors, and ENM (elastic network model) to check the deformation and variance in protein movement [60].

2.14. Disulfide engineering of the candidate vaccine

Disulfide engineering is creating disulfide bonds between two

adjacent protein chains which in turn increases the stability of the protein [61]. Using the technique, the structure of the vaccine can be improved further. Therefore, we performed the disulfide engineering of the candidate vaccine structure with Disulphide by Design v2.12 web-platform [62]. To accomplish this, we submitted the refined model for searching suitable residue pairs for potential disulfide bridging locations. As recommended by the server, the energy value ≤ 2.2 and the $-87 \leq X^3 \leq +97$ were considered suitable and promising locations for disulfide bridging.

2.15. Conformational B-cell epitope prediction

The conformational (discontinuous) B-cell epitope (CBE) is the 3D location in the protein structure that can bind to the specific paratope, thereby, generating the humoral immune response. Therefore, the presence of CBE on the vaccine protein is important. We employed the ElliPro tool available in the IEDB server to determine the CBE. The tool utilizes three algorithms to estimate the protein's 3D structure, residue's protrusion scale, and neighboring residues of the cluster. The ElliPro produced an average protrusion value for each epitope in which 0.9 is considered to contain 90% of residues while the rest 10% residues are outside of the ellipsoids [42].

3. Results

3.1. The highly Antigenic proteins

To identify the potential antigens, a total of 521 protein sequences were retrieved from the ViPR database that are derived from CCHFV. As we stated earlier, proteins are primarily grouped into several classes, including glycoprotein, glycoprotein precursor, envelope glycoprotein, envelope glycoprotein precursor, pre-glycoprotein, and membrane glycoprotein. All of these proteins are structural proteins that are important in the viral invasion. We predicted the antigenicity for proteins included in all classes with 0.5 cut off value. In addition, the adhesion score ≥ 0.5 were considered antigen with "high potential", while those with a score of 0.4–0.5 were considered antigens with "intermediate potential". Finally, we selected the highest antigenic protein from each class, as provided in Table 1.

3.2. Potential CD8⁺, CD4⁺, and LBC epitopes

A total of 283 unique CD8⁺ epitopes (9AA each) were identified initially. Among all, 140 epitopes were antigenic and immunogenic without allergenic and toxic properties in which 66 epitopes had antigenicity score more than 1 (Table S1). We considered the top 6 antigenic CD8⁺ epitopes from different GP classes (Table 2). Similarly, a total of 23 unique CD4⁺ epitopes (15AA each) and their respective MHC-II alleles (Table S2). Upon evaluation, we selected 3 CD4⁺ epitopes that are capable of provoking 3 categories of cytokines, i.e., IL-4, IFN- γ , and IL-10 (Table 3). Among the predicted 2797 epitopes, we only selected 7 unique LBC epitopes with higher antigenicity, non-allergenicity, and non-toxicity (Tables 4 and Table S3).

Table 1
List of different glycoproteins with the highest antigenic scores.

| Protein name | Antigenic score | GenBank ID |
|---------------------------------|-----------------|------------|
| Envelope glycoprotein | 0.5358 | AAW84284.1 |
| Envelope glycoprotein precursor | 0.5445 | AAK18286.1 |
| Glycoprotein | 0.5496 | AIE16132.1 |
| Glycoprotein precursor | 0.5380 | ARB51452.1 |
| Membrane glycoprotein | 0.5002 | ABA39298.1 |
| Pre-glycoprotein | 0.5169 | ADD64467.1 |

3.3. Worldwide coverage of candidate vaccine

We estimated the population coverage of the selected epitopes for various geographic locations of the world. Interestingly, our chosen CD8⁺ and CD4⁺ epitopes cover 81.23 and 81.94% of the world's population, respectively (Tables S4–6). In combination, they provided 96.61% population coverage. Importantly, our vaccine covers the population of East Asia, Central Africa, East Africa, South Asia, West Africa, South Africa, Europe, Turkey, and Russia by 86.34, 89.75, 95.81, 78.82, 91.80, 89.66, 98.16, 87.86, and 94.62%, respectively (Fig. 1A). Furthermore, the selected epitopes cover 91.17% population of Chile, 86.17% of China, 90.45% of India, and more than 90% of populations in 202 other countries (Table S4).

3.4. Epitope-based peptide vaccine

Using the previously selected epitopes, we orchestrated a multi-epitope vaccine. In doing so, CD8⁺ epitopes were incorporated with AAY linkers, while CD4⁺ epitopes were integrated by GPGPG linkers. Contrastingly, LBC epitopes were merged by KK linkers. For better immunogenic potency, we also added LprG protein as an adjuvant. This protein is a TLR2 agonist having 236 amino acids and added in front of the construct using the EAAAK linker. Thus, the final chimeric protein consists of 468 AA residues. The graphical illustration of the multi-epitope vaccine construct is shown in Fig. 1B.

3.5. Physicochemical and immunological properties

We evaluated the designed construct in terms of physicochemistry and immunology. Table 5 shows the different properties of the chimera protein, including MW (50.08 kDa) theoretical pI (9.58), II (20.62), AI (85.94), and GRAVY (-0.270). In addition, other properties are included in Table 5. On the other hand, the immunogenic evaluation revealed that the constructed chimera vaccine is antigenic (0.62) and non-allergenic as well as soluble in nature (Table 5).

3.6. Secondary and tertiary structure

The secondary structural features of the vaccine include 30.12% α -helix (141 residues), 28% β -strand (131 residues), and 41.88% random coil (196 residues). Later, we modelled our vaccine using I-TASSER server. Among the 5 generated models, the quality indicator C-score was ranged in between -3.01 and -0.58. C-score usually ranged within -5 to 2 in which higher value indicates a better structure. Despite the suitability of structure with a high C-score, we selected model 5 (Fig. 1C) that has a C-score of -3.01 due to the low-quality folding and reduced compactness in other models.

3.7. Refinement and validation of vaccine model

The structural refinement provided 5 models with different magnitude of structural optimization.

Among all the refined models, we considered the model 1 as the best based on its properties. For instance, Rama favor was 92.1% while other properties were also in the acceptable range, such as 0.9274 of GDT-HA and 0.485 of RMSD, etc. (Tables S7–8). Further, we used RAMPAGE and ProSA-web to validate the structural refinement. The Ramachandran plot showed 92.1% of residues are located in the energy-favored region, 5.8% in allowed, and 2.1% of residues were located in the outlier region (Fig. 1D). On the other hand, overall model quality Z-score of -7.55 indicates that the overall quality of the structure falls in the region on X-ray-derived structure (Fig. 1E).

3.8. Binding affinity between vaccine and TLR2 receptor

We performed molecular docking between the vaccine and TLR2

Table 2Immunological properties of CD8⁺ epitopes selected for mapping vaccine construct.

| Protein | Epitope | Location | C-score | Antigenicity | Immunogenicity | Allergenicity | Toxicity |
|---------------------------------|-----------|-----------|---------|--------------|----------------|---------------|----------|
| Membrane glycoprotein | TSITVQDTY | 229–239 | 1.1803 | 1.4672 | 0.05482 | No | No |
| | TQHNHAAFV | 1378–1388 | 0.5393 | 1.0775 | 0.17374 | No | No |
| Envelope glycoprotein precursor | LEMEIILTL | 253–263 | 0.7055 | 1.0377 | 0.31195 | No | No |
| | KAGCWESV | 1573–1583 | 1.031 | 1.1034 | 0.14985 | No | No |
| Envelope glycoprotein | IEFGADSTF | 1511–1521 | 0.5052 | 1.1469 | 0.01414 | No | No |
| | FQIYHVGNL | 1330–1340 | 0.5637 | 1.2269 | 0.13466 | No | No |

Table 3Immunological properties of CD4⁺ epitopes selected for mapping of vaccine construction.

| Protein | Epitope | Location | Antigenicity | Interleukin-4 | Interleukin-10 | Interferon- γ |
|-----------------------|-----------------|----------|--------------|---------------|----------------|----------------------|
| Pre-Glycoprotein | QGLKKYYSKILKLLQ | 271–287 | 0.9621 | Inducer | Inducer | Positive |
| | NKALLIRSIINSTFV | 978–994 | 1.3121 | Inducer | Inducer | Positive |
| Membrane Glycoprotein | ELGCYTINRVKSFKL | 573–589 | 0.9621 | Inducer | Inducer | Positive |

Table 4

Immunological properties of LBC epitopes selected for mapping of vaccine construction.

| Protein | Epitope | Location | Probability | Antigenicity | Allergenicity | Toxicity |
|---------------------------------|--------------|----------|-------------|--------------|---------------|----------|
| Pre-glycoprotein | EITTKNSPPTAG | 186–199 | 0.8407 | 1.14 | No | No |
| | LNLERIPWLVRK | 806–819 | 0.853 | 1.3906 | No | No |
| Envelope glycoprotein precursor | LKDNLIDLGCPN | 662–675 | 0.824 | 1.1781 | No | No |
| | QYRTEIKIGKAS | 505–518 | 0.8019 | 1.0837 | No | No |
| Glycoprotein | LSVTSTKPGETP | 154–167 | 0.8135 | 1.324 | No | No |
| | IVIDKKDKQNDR | 471–884 | 0.8085 | 1.6808 | No | No |
| Membrane glycoprotein | TSITVQDTPSP | 229–242 | 0.8209 | 1.3932 | No | No |

immune-related protein using the ClusPro v2.0 web-server. After docking operation, the server produced a total of 30 docked complex with different binding poses (Table S9). In docking studies, binding interaction that required minimal energy is considered as the best-docked pose. Therefore, we selected the model 3 as it is provided the lowest energy score –1278.7 and properly bound to the active site of the TLR2 protein. Fig. 1F provides a graphical representation of the best-docked state of our vaccine-TLR2 complex by marking the specific clusters.

3.9. Codon optimization and *in silico* cloning

In silico cloning is the expression of the recombinant vaccine in a suitable host organism. Herein, we used *E. coli* strain K12 as our target host system for prospective vaccine production. The length of the optimized codon sequence was 1,404 nucleotides with 51.64% of GC content and 0.966 of CAI value. Later on, two restriction sites such *Xba*I and *Nde*I were generated and cloned into the plasmid vector pET28a (+) using SnapGene software. A circular map of the CCHFV vaccine clone is provided in Fig. 1G. After successful insertion, the total length of the expression vector, along with the vaccine DNA was 6.7 kbp.

3.10. Immune response dynamics

The immune response generated *in silico* was consistent with the actual immune response. For example, significantly higher secondary and tertiary immune reactions than that of the initial response. The ordinary elevated concentrations of immunoglobulin (Ig) activities (i.e., IgG1+IgG2, IgM, and IgG + IgM antibodies) were apparent with a reduction in the amount of antigens (Fig. 2A). In addition, B-lymphocyte isotypes were observed with long-standing activity suggesting their potentiality in switching isotypes and the memory cell development (Fig. 2B and C). A likewise elevated reaction has been noticed in populations of helper T-lymphocytes (TH) and cytotoxic T-lymphocytes (TC) with effective memory development (Fig. 2D and E). Furthermore, elevated activity of macrophage was shown during exposure, while continuous dendritic-cell (DC) activity was evident (Fig. 2F and G).

Moreover, prominent activities of different cytokines, especially IFN- α and IL-2 concentrations, were also apparent (Fig. 2H). Moreover, a smaller Simpson index (D) suggests a diversity of the immune responses.

3.11. Structural stability of the vaccine-TLR2 complex

In this study, software-based MD simulation was executed where trajectories derived in 5 ns long MD simulation provided structural stability around 3.5 ns and very little fluctuation afterward (Fig. 3A and Table S10). The average RMSD value was calculated to be 2.78 Å, and RMSF of 4.11 Å. The movement was little bit higher in the vaccine portion from AA₅₇₀ to AA₁₀₁₇ (Fig. 3B). Furthermore, the estimation of overall energy of the simulation was –7261872.45 kJ/mol while the overall Rg value was 38.07 fluctuating within 32.92 and 43.78 (Fig. 3C). The relatively higher pick at AA₅₇₀ to AA₁₀₁₇ is due to the tensile regions (vaccine part) of the vaccine-TLR2 complex. In addition, the MD simulation studies were performed in the iMODS web-tool in which NMA evaluation was employed to the complex's internal coordinates. The deformability aggravated the independent residual distortion portrayed by the chain hinges (Fig. 3D). Herein, the calculated eigenvalue for the docked-complex was found to be 2.24e-06 (Fig. 3E). The variance in each mode was gradually decreased with the increment of modes (Fig. 3F). Altogether, these results indicate steady binding relationship with compact structural conformation as well as little atomic movement in the docked complex.

3.12. Disulfide bridging for vaccine stability

By using the Disulfide by Design v2.12 web-tool, a total of 31 pairs of amino acid residues were found that are opted for disulfide engineering (Table S11). After evaluation, we identified only 4 residue pairs having the potential feature to be engineered. We considered the energy score ≤ 2.2 kcal/mol and χ^3 angle in within –87 and +97°. Therefore, a total of eight mutations were created on the residue-pairs. For Trp120-Pro233 residual pair, the energy score is 1.73 kcal/mol and the χ^3 angle is 90.36°, Asp210-Ser216 residual pair with energy score 1.85 kcal/mol

and the $\gamma 3$ angle 92.89°, Ala41-Ala152 residual pair with energy score 1.89 kcal/mol and the $\gamma 3$ angle 87.33°, and His59-Lys223 residual pair with energy score 2.13 kcal/mol and the $\gamma 3$ angle 101.18°. These residue-pairs were altered to Cysteine (C) residue pairs to facilitate the disulfide bridging between them as shown in Fig. 4A.

3.13. Conformational B-cell epitopes in vaccine

The prediction of conformational B-cell epitopes was made with the ElliPro web-server. A total of 260 residues were anticipated to be situated in 5 locations on the surface of the vaccine's 3D structure (Table S12). Thus, 5 discontinuous B-cell epitopes were predicted and score ranges from 0.511 to 0.746 as shown in Fig. 4. The size of the epitopes ranged from 3 to 77 residues.

4. Discussion

The vaccine is the most promising way to develop immunity against specific pathogens [63]. Despite the viral outbreaks in recent times, however, no vaccination is available that can prevent CCHFV infection. The development of the CCHFV vaccine is very challenging because of the error-prone nature of CCHFV polymerase, high infection rate, and lack of appropriate animal model [1]. In addition, efficient progression and manufacturing of vaccines are expensive and can take years to complete. Immunoinformatics can eliminate this workload by the implementation of multiple server-based tools and databases to predict potential epitopes of B- and T-cells that can be tailored into a potent vaccine candidate [64,65]. In this study, we used recently advanced techniques in computational immunology to predict potential immunodominant epitopes in antigenic proteins from CCHFV proteome,

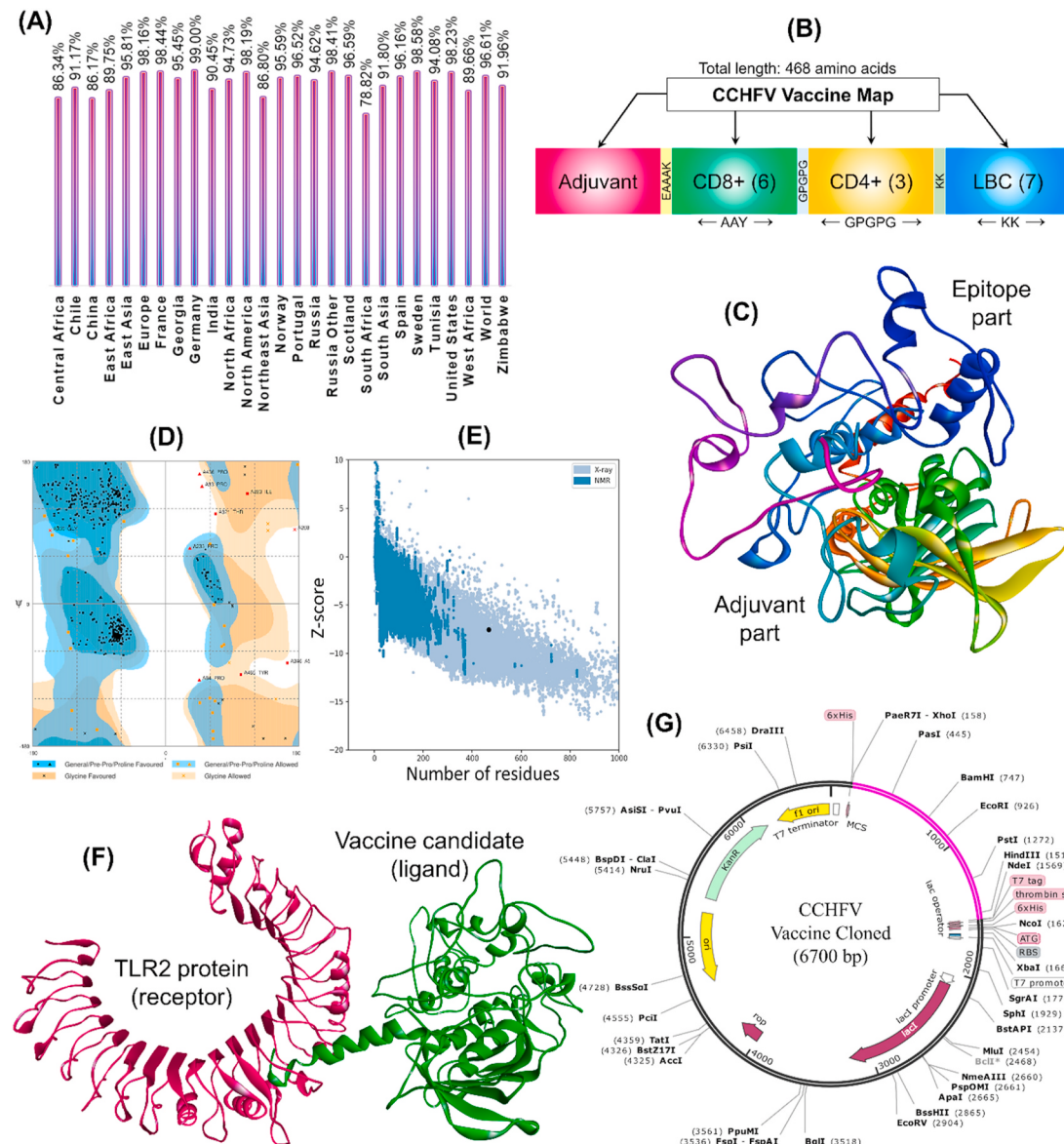


Fig. 1. Population coverage, design, and evaluation of vaccine candidate. (A) region-wise % of population coverage by included CD8⁺ and CD4⁺ epitopes and their corresponding HLA alleles; (B) Construction of epitope-based chimeric vaccine that includes an adjuvant, T-cell & B-cell epitopes, and linkers. The adjuvant was added to the N-terminal end using EAAAK linker while CD8⁺, CD4⁺, and LBC epitopes were fused together with AAY, GPGPG, and KK linkers; (C) tertiary (3D) structure of the vaccine construct (D) Ramachandran plot statistics showing the % of most favored (92.1%), allowed (5.8%), and outlier regions (2.1%) of the vaccine; (E) Z-score of -7.55 indicate the X-ray-like structural quality of the vaccine protein; (F) docking simulation between vaccine candidate (pink color) into pET28a (+) expression vector (black color) by placing the vaccine's DNA between *Xba*I (158) and *Nde*I (1569) restriction sites.

Table 5
Primary sequence evaluation of the chimera vaccine protein.

| Features | Assessment |
|--|--|
| Number of residues | 468 |
| Molecular weight | 50.08 kDa |
| Chemical formula | C ₂₂₃₇ H ₃₆₀₈ N ₆₁₄ O ₆₆₈ S ₉ |
| Theoretical pI | 9.58 |
| Number of negative charge residues (Asp + Glu) | 37 |
| Number of positive charge residues (Arg + Lys) | 58 |
| Number of total atoms | 7136 |
| Extinction coefficient (at 280 nm in H ₂ O) | 48,610 M ⁻¹ cm ⁻¹ |
| Instability index (II) | 20.62 |
| Aliphatic index (AI) | 85.94 |
| Grand average of hydropathicity (GRAVY) | -0.270 |
| Antigenicity | 0.6211 |
| Allergenicity | Non-allergen |
| Solubility | 0.548 |

followed by the designing of a potent vaccine candidate.

In previous studies, epitopes for vaccine design were predicted from either RdRP or glycoprotein precursor [1,27]. Conversely, we have considered several structural proteins as the epitope source while designing a vaccine candidate to facilitate more specificity. In addition, we included both B- and T-cell epitopes in designing our vaccine so that it can induce both antibody and cell-dependent immunities. The peptide vaccine construct has 468 residues and was found to be stable at 9.58 pH range, while the negative GRAVY index supports its good interaction with water. Furthermore, the vaccine was stable at normal and high

temperatures. Interestingly, the epitopes considered in the vaccine protein showed 96.61% of global population coverage. It is mention-worthy that our vaccine covers even more than 95% of the inhabitants in CCHFV outbreaks areas. Therefore, this vaccine candidate could probably be effective for the majority of the world population. Most importantly, the immunological evaluation suggests that the vaccine candidate has the potentiality to induce an immune response without producing an allergic reaction. For the post-production process such as purification, solubility upon overexpression is very important [66]. Luckily, our vaccine construct was highly soluble indicating easy purification.

We applied a multistep process for refinement and structural validation of the vaccine candidate to ensure its good quality. Ramachandran statistics were used to measure the energetically favored residues and Z-score for overall quality based on the X-ray and NMR-derived validated protein structure. For instance, in crude 3D vaccine protein, 74.0% residues were in Rama favored area, whereas the refined model has as much as 92.1%. In general, a good quality model is likely to have at least 90% of the total residues in the favored region [67]. Likewise, overall quality indicator Z-score (-7.55) suggests that our vaccine structure was similar to the X-ray crystallized structures. A vaccine designed by Nosrati et al. had 73.4% of residues in the favored region and Z-score of -1.74 in its refined form [1]. This clearly shows that our vaccine candidate is more close to the native structure as well as more compact. Furthermore, CAI score and GC content of the vaccine were 0.97 and 51.64%, respectively. The ideal CAI score is close to the ideal

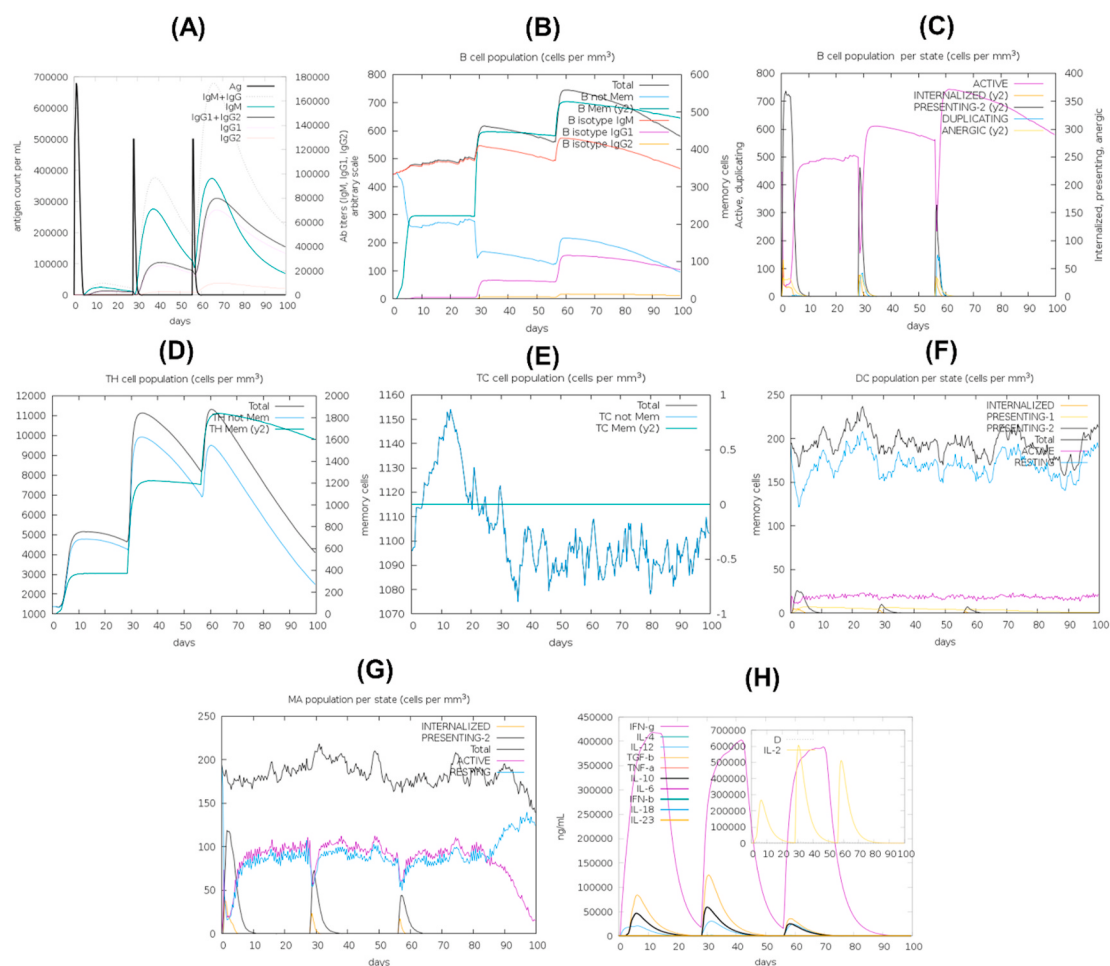


Fig. 2. Immune simulation response triggered by the vaccine antigen. Plots show the state of different immune cells where (A) pattern of immune responses upon antigen exposure, (B) B-cell population indicating memory cell formation, (C) state-wise B-lymphocyte populations (D) helper T-lymphocyte population, (E) cytotoxic T-lymphocyte population, (F) state-wise DC population, (G) state-wise macrophage population, and (H) cytokine production and diversity assessment.

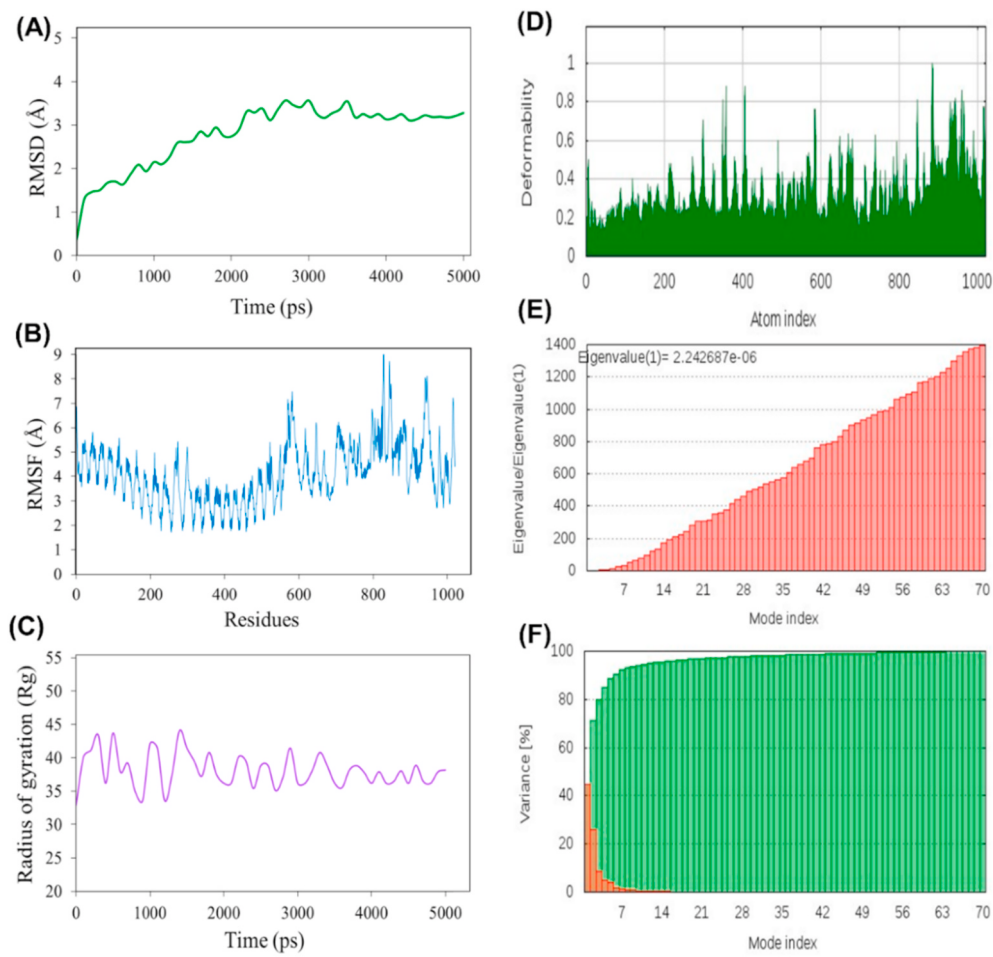


Fig. 3. Simulation of vaccine-TLR2 complex's molecular dynamics. Herein, various MD simulation plots showing complex's (A) RMSD as the stability, (B) RMSF as the structural integrity, (C) R_g as the protein compactness, (D) residual hinges as deformability, (E) difference of eigenvalue as motion stiffness, and (F) variance in normal modes.

score 1.0, which indicates the higher probability of expression in the vector system. Altogether, our designed vaccine is seemed to be an excellent candidate.

For efficient transportation into the human body, vaccine candidates should endure strong affinity towards the immune-related receptors [68]. This study revealed robust interactions in molecular docking between the TLR2 protein and vaccine, where minimal energy for efficient binding is required. Furthermore, during MD simulation, the vaccine-TLR2 complex has been observed to be steady where some tiny-changes and mild movement of the protein backbone were found in the flexible/tensile regions [61,69]. These results are consistent with an earlier study in which the docked complex was stabilized in a similar time-scale [19,69,70]. The vaccine-TLR2 compactness was also supported by the R_g score. The eigenvalue associated with each normal mode reflects the rigidity of motion and is correlated with the required energy for deforming the structure. The lower the eigenvalue, the easier to be deformed [60]. In our server-based NMA analysis, there was a gradual increase in eigenvalue, which indicates protein stability and compactness. The vaccine's stability was further improved by disulfide bridging. Our data, therefore, suggest that the constructed vaccine candidate will be able to generate robust and stable contacts with the immune proteins.

Immune reaction differs according to viral pathogenesis and the host's defense system. For example, immunity against CCHFV was thought to depend on the robust development of IgG and IgM antibodies [71]. Recent studies suggest that T-cell immunity plays a crucial role for effective protection against CCHFV. In addition, IFN pathways are also

important to control CCHFV pathogenesis [72]. In our study, the simulated immune response showed an abundance of B-and T-cells, especially enriched with helper T-cells, which indicates the vaccine candidate will be able to provide good protection. Moreover, an elevated amount of IL-2 and IFN- γ was evident, which may block the pathogenic invasion. Moreover, the activity of antigen-presenting cells (APC) such as macrophage and DC populations were satisfactory. The lower level of D value indicates the diversity of the immune responses [57]. The induction of both immunoglobulins and T-cell immune reactions with greater diversity is plausible as it contains both B and T-cell epitopes. In immunoinformatics, there are some certain drawbacks. Therefore, it is not possible to portray the efficiency and specificity of the designed vaccine in actual biological systems. However, in light of our findings, we believe that the proposed chimera protein can be a potential vaccine candidate for further *in vivo* and *in vitro* assessments.

5. Conclusion

In recent years, CCHFV outbreaks occurred in several countries and it has been marked as a burning issue in medical science because of its mortality rate, absence of prospective medicines, and lack of an efficient vaccine. On the other side, the building of peptide-based vaccines also became evident because of its benefits. With the assistance of immunoinformatics and bioinformatics, this multiepitope design research focuses on elucidating possible efficient peptide vaccines that could provide immunity to CCHFV. Antigenic as well as immunogenic T- and B-cell epitopes were mapped and tested for their higher conservancy and

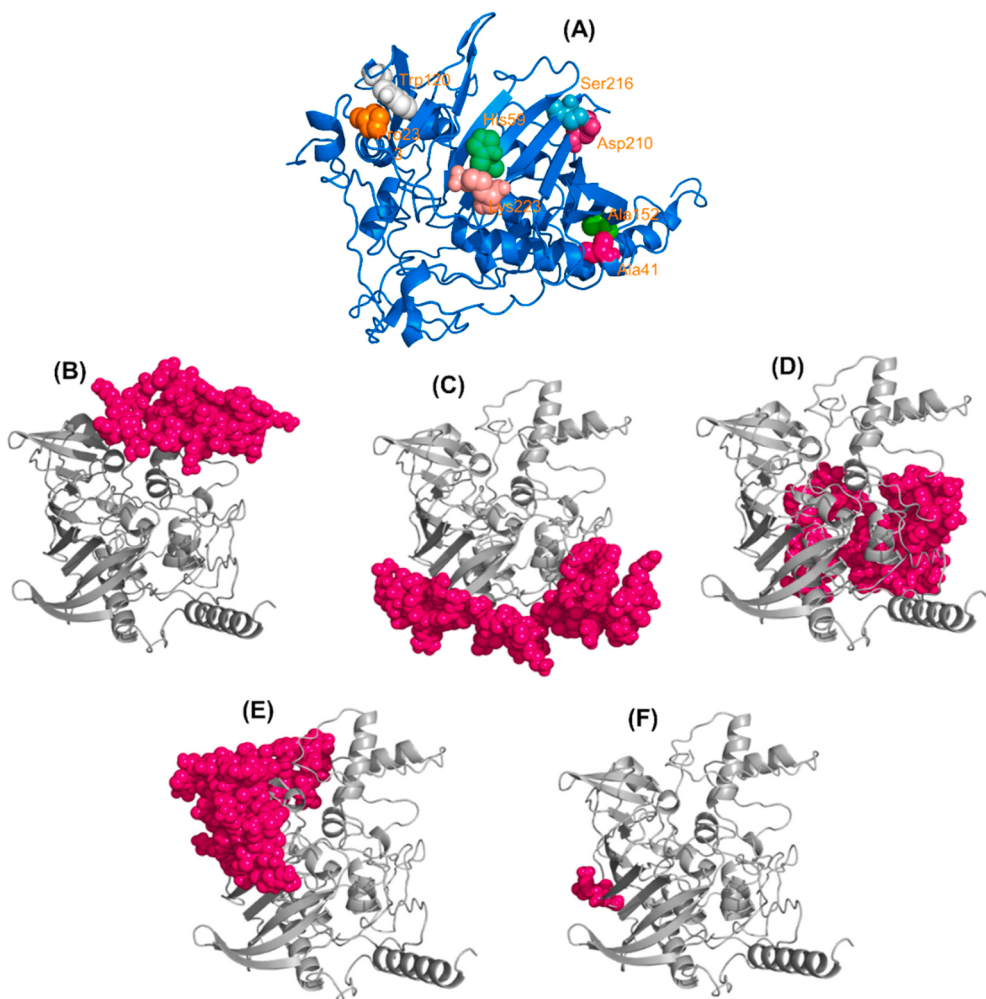


Fig. 4. Residues for disulfide bridging and conformational B-cell epitopes. The vaccine contains (A) four mutated residue pairs shown in red-green, pink-cyan, pink-green, and orange-white colored spheres and five B-cell epitopes where (B) 45 residues with 0.746, (C) 77 residues with 0.712, (D) 75 residues with 0.673, (E) 60 residues with 0.658, and (F) 3 residues with 0.511 scores. Herein, the epitopic regions are indicated by pink-colored spheres.

immunological properties. Significant interaction with MHC allele with good affinity has been considered to produce an effective vaccine. We also performed molecular docking and immune simulation to detect the effectiveness of the vaccine. This information minimizes the efforts in the laboratory and offers a definite concept for studies on epitope-based peptide vaccine research.

CRediT Contributions

Md. Shakil Ahmed Khan: Conceptualization, Formal analysis, Investigation, Writing - original draft, Visualization. Zulkar Nain: Conceptualization, Formal analysis, Writing - original draft preparation, Writing - review & editing, Project administration. Shifath Bin Syed: Formal analysis, Writing - original draft preparation. Faruq Abdulla: Writing - review & editing. Md. Mohiuddin Sheam: Formal analysis, Writing - original draft preparation. Mohammad Ali Moni: Writing - review & editing. Mohammad Minnatul Karim: Writing - review & editing, Supervision. Utpal Kumar Adhikari: Conceptualization, Methodology, Writing - review & editing, Supervision. All authors reviewed the revised manuscript and approved the revised manuscript for publication in the journal of Molecular and Cellular Probes.

Funding

Not applicable.

Declaration of competing interest

The authors declare no conflict of interest.

Appendix A. Supplementary data

Supplementary data to this article can be found online at <https://doi.org/10.1016/j.mcp.2020.101693>.

References

- [1] M. Nosrati, M. Behbahani, H. Mohabatkar, Towards the first multi-epitope recombinant vaccine against Crimean-Congo hemorrhagic fever virus: a computer-aided vaccine design approach, *J. Biomed. Inf.* (2019) 103160, <https://doi.org/10.1016/j.jbmi.2019.103160>.
- [2] S.S. Karti, Z. Odabasi, V. Korten, M. Yilmaz, M. Sonmez, R. Caylan, E. Akdogan, N. Eren, I. Koksal, E. Ovali, B.R. Erickson, M.J. Vincent, S.T. Nichol, J.A. Comer, P. E. Rollin, T.G. Ksiazek, Crimean-Congo Hemorrhagic Fever in Turkey 10 (2004) 1379–1384.
- [3] P. Emmerich, A. Mika, R. Von Posse, A. Rackow, Y. Liu, K. Sherifi, B. Halili, X. Jakupi, H. Schmitz, S. Gu, L. Berisha, S. Ahmeti, C. Deschermeier, Sensitive and Specific Detection of Crimean-Congo Hemorrhagic Fever Virus (CCHFV)—Specific IgM and IgG Antibodies in Human Sera Using Recombinant CCHFV Nucleoprotein as Antigen in μ -capture and IgG Immune Complex (IC) ELISA Tests, 2018, pp. 1–24.
- [4] J.P. Messina, D.M. Pigott, N. Golding, K.A. Duda, J.S. Brownstein, D.J. Weiss, M. F. Myers, D.B. George, S.I. Hay, The global distribution of Crimean-Congo hemorrhagic fever, Crime Congo Hemorrhagic Fever (2015) 1–11, <https://doi.org/10.1093/trstmh/trv050>.

- [5] O. Ergonul, Crimean – Congo hemorrhagic fever virus : new outbreaks , new discoveries, *Curr. Opin. Virol.* 2 (2012) 215–220, <https://doi.org/10.1016/j.coviro.2012.03.001>.
- [6] S. Aslam, M.S. Latif, M. Daud, Z.U. Rahman, B. Tabassum, M.S. Riaz, A. Khan, M. Tariq, T. Husnain, Crimean-Congo hemorrhagic fever: risk factors and control measures for the infection abatement (Review), *Biomed. Reports.* 4 (2016) 15–20, <https://doi.org/10.3892/br.2015.545>.
- [7] R. Flick, C.A. Whitehouse, S. Division, U. States, D. Usamriid, Crimean-Congo Hemorrhagic Fever Virus, 2005, pp. 753–760.
- [8] A.J. Sanchez, M.J. Vincent, S.T. Nichol, Characterization of the glycoproteins of crimean-Congo hemorrhagic fever, *Virus* 76 (2002) 7263–7275, <https://doi.org/10.1128/JVI.76.14.7263>.
- [9] A. Fritzen, C. Risinger, G. Korukluoglu, I. Christova, A. Corli Hitzeroth, N. Viljoen, F.J. Burt, A. Mirazimi, O. Blixt, Epitope-mapping of the glycoprotein from Crimean-Congo hemorrhagic fever virus using a microarray approach, *PLoS Neglected Trop. Dis.* 12 (2018) 1–15, <https://doi.org/10.1371/journal.pntd.0006598>.
- [10] D.M. Watts, M.A. Ussery, D. Nash, C.J. Peters, Inhibition of crimean-Congo hemorrhagic fever viral infectivity yields in vitro by ribavirin, *Am. J. Trop. Med. Hyg.* (1989), <https://doi.org/10.4269/ajtmh.1989.41.581>.
- [11] Z. Arab-Bafrahi, A. Jabbari, M. Mostakhdem Hashemi, A.M. Arabzadeh, A. Gilaniopur, E. Mousavi, Identification of the crucial parameters regarding the efficacy of ribavirin therapy in Crimean-Congo haemorrhagic fever (CCHF) patients: a systematic review and meta-analysis, *J. Antimicrob. Chemother.* (2019), <https://doi.org/10.1093/jac/dkz328>.
- [12] C.A. Whitehouse, Crimean – Congo hemorrhagic fever 64 (2004) 145–160, <https://doi.org/10.1016/j.antiviral.2004.08.001>.
- [13] M. Keshtkar-Jahromi, J.H. Kuhn, I. Christova, S.B. Bradfute, P.B. Jahrling, S. Bavari, Crimean-Congo hemorrhagic fever: current and future prospects of vaccines and therapies, *Antivir. Res.* 90 (2011) 85–92, <https://doi.org/10.1016/j.antiviral.2011.02.010>.
- [14] A.R. Garrison, C.J. Shoemaker, J.W. Golden, C.J. Fitzpatrick, J.J. Suschak, M. J. Richards, C. V Badger, C.M. Six, J.D. Martin, D. Hannaman, M. Zivec, E. Bergeron, W. Koehler, C.S. Schmaljohn, A DNA Vaccine for Crimean-Congo Hemorrhagic Fever Protects against Disease and Death in Two Lethal Mouse Models, 2017, pp. 1–19.
- [15] S. Devignot, E. Bergeron, S. Nichol, A. Mirazimi, F. Weber, A virus-like particle system identifies the endonuclease domain of crimean-Congo hemorrhagic fever virus, *J. Virol.* 89 (2015) 5957–5967, <https://doi.org/10.1128/jvi.03691-14>.
- [16] A.J. Sanchez, M.J. Vincent, B.R. Erickson, S.T. Nichol, Crimean-Congo hemorrhagic fever virus glycoprotein precursor is cleaved by furin-like and SKI-1 proteases to generate a novel 38-kilodalton glycoprotein, *J. Virol.* 80 (2006) 514–525, <https://doi.org/10.1128/jvi.80.1.514-525.2006>.
- [17] P. Taylor, S.D. Dowall, K.R. Buttigieg, E. Rayner, G. Pearson, A. Miloszewska, Human Vaccines & Immunotherapeutics A Crimean-Congo Haemorrhagic Fever (CCHF) viral vaccine expressing nucleoprotein is immunogenic but fails to confer protection against lethal disease A Crimean-Congo Haemorrhagic Fever (CCHF) viral vaccine expressin, <https://doi.org/10.1080/21645515.2015.1078045>, 2015.
- [18] J. Kortekaas, R.P.M. Vloet, A.J. McAuley, X. Shen, B.J. Bosch, L. De Vries, R.J. M. Moormann, D.A. Bente, Crimean-Congo hemorrhagic fever virus subunit vaccines induce high levels of neutralizing antibodies but no protection in STAT1 knockout mice, *Vector Borne Zoonotic Dis.* 15 (2015) 759–764, <https://doi.org/10.1089/vbz.2015.1855>.
- [19] Z. Nain, F. Abdulla, M.M. Rahman, M.M. Karim, M.S.A. Khan, S. Bin Sayed, S. Mahmud, S.M.R. Rahman, M.M. Sheam, Z. Haque, U.K. Adhikari, Proteome-wide screening for designing a multi-epitope vaccine against emerging pathogen Elizabethkingia anophelis using immunoinformatic approaches, *J. Biomol. Struct. Dyn.* (2019) 1–18, <https://doi.org/10.1080/07391102.2019.1692072>.
- [20] Z. Nain, M.M. Karim, M.K. Sen, U.K. Adhikari, Structural basis and designing of peptide vaccine using PE-PGRS family protein of Mycobacterium ulcerans—an integrated vaccinomics approach, *Mol. Immunol.* 120 (2020) 146–163, <https://doi.org/10.1016/j.molimm.2020.02.009>.
- [21] S. Bin Sayed, Z. Nain, M.S.A. Khan, F. Abdulla, R. Tasmin, U.K. Adhikari, Exploring lassa virus proteome to design a multi-epitope vaccine through immunoinformatics and immune simulation analyses, *Int. J. Pept. Res. Therapeut.* (2020), <https://doi.org/10.1007/s10989-019-10003-8>.
- [22] R.K. Pandey, T.K. Bhattacharya, V.K. Prajapati, Novel immunoinformatics approaches to design multi-epitope subunit vaccine for malaria by investigating Anopheles salivary protein, *Sci. Rep.* 8 (2018) 1125, <https://doi.org/10.1038/s41598-018-19456-1>.
- [23] N. Nezafat, Z. Karimi, M. Eslami, M. Mohkam, S. Zandian, Y. Ghasemi, Designing an efficient multi-epitope peptide vaccine against Vibrio cholerae via combined immunoinformatics and protein interaction based approaches, *Comput. Biol. Chem.* 62 (2016) 82–95, <https://doi.org/10.1016/j.combiolchem.2016.04.006>.
- [24] H. Dorost, M. Eslami, M. Negahdaripour, M.B. Ghoshoon, A. Gholami, R. Heidari, A. Dehshahr, N. Erfani, N. Nezafat, Y. Ghasemi, Vaccinomics approach for developing multi-epitope peptide pneumococcal vaccine, *J. Biomol. Struct. Dyn.* 37 (2019) 3524–3535, <https://doi.org/10.1080/07391102.2018.1519460>.
- [25] R.A. Shey, S.M. Ghogomu, K.K. Esoh, N.D. Nebangwa, C.M. Shintouo, N. F. Nongley, B.F. Asa, F.N. Ngale, L. Vanhamme, J. Souoogui, In-silico design of a multi-epitope vaccine candidate against onchocerciasis and related filarial diseases, *Sci. Rep.* 9 (2019) 4409, <https://doi.org/10.1038/s41598-019-40833-x>.
- [26] A. Ali, A. Khan, A.C. Kaushik, Y. Wang, S.S. Ali, M. Junaid, S. Saleem, W.C.S. Cho, X. Mao, D. Wei, Immunoinformatic and systems biology approaches to predict and validate peptide vaccines against Epstein – barr virus (EBV), *Sci. Rep.* (2019) 1–12, <https://doi.org/10.1038/s41598-018-37070-z>.
- [27] D. Press, Identification of Highly Conserved Regions in L-Segment of Crimean – Congo Hemorrhagic Fever Virus and Immunoinformatic Prediction about Potential Novel Vaccine, 2015, pp. 1–10.
- [28] B.E. Pickett, E.L. Sadat, Y. Zhang, J.M. Noronha, R.B. Squires, V. Hunt, M. Liu, S. Kumar, S. Zaremba, Z. Gu, L. Zhou, C.N. Larson, J. Dietrich, E.B. Klem, R. H. Scheuermann, ViPR : an open bioinformatics database and analysis resource for virology research, *Nucleic Acids Res.* 40 (2012) 593–598, <https://doi.org/10.1093/nar/gkr859>.
- [29] Y. Hisham, Y. Ashhab, Identification of Cross-Protective Potential Antigens against Pathogenic Brucella Spp . Through Combining Pan-Genome Analysis with Reverse Vaccinology, 2018, p. 2018.
- [30] I.A. Doytchinova, D.R. Flower, VaxiJen: a server for prediction of protective antigens, tumour antigens and subunit vaccines, *BMC Bioinf.* 8 (2007) 4, <https://doi.org/10.1186/1471-2105-8-4>.
- [31] M. V Larsen, C. Lundsgaard, K. Lambeth, S. Buus, O. Lund, M. Nielsen, Large-scale validation of methods for cytotoxic T-lymphocyte epitope prediction, *BMC Bioinf.* 8 (2007) 424, <https://doi.org/10.1186/1471-2105-8-424>.
- [32] M. Moutaftsi, B. Peters, V. Pasquetto, D.C. Tscharke, J. Sidney, H. Bui, H. Grey, A. Sette, A consensus epitope prediction of murine T CD8 + -cell responses to vaccinia virus, (n.d.) 817–819, <https://doi.org/10.1038/nbt1215>.
- [33] A.G. Leroux-roels, P. Bonanni, Vaccine development, *Perspect. Vaccinol.* 1 (n.d.) 115–150, <https://doi.org/10.1016/j.pervac.2011.05.005>.
- [34] J.J.A. Calis, M. Maybeno, J.A. Greenbaum, D. Weiskopf, A.D. De Silva, A. Sette, C. Keşmir, B. Peters, Properties of MHC class I presented peptides that enhance immunogenicity, *PLoS Comput. Biol.* 9 (2013), e1003266, <https://doi.org/10.1371/journal.pcbi.1003266>.
- [35] I. Dimitrov, L. Naneva, I. Doytchinova, I. Bangov, Systems biology AllergenFP : allergenicity prediction by descriptor fingerprints, *Bioinformatics* (2013) 1–6, <https://doi.org/10.1093/bioinformatics/btt619>.
- [36] S. Gupta, P. Kapoor, K. Chaudhary, A. Gautam, R. Kumar, G.P.S. Raghava, G.P. S. Raghava, In silico approach for predicting toxicity of peptides and proteins, *PLoS One* 8 (2013), e73957, <https://doi.org/10.1371/journal.pone.0073957>.
- [37] M. Nielsen, O. Lund, Algorithm for MHC class II peptide binding prediction, *BMC Bioinf.* 10 (2009) 1–10, <https://doi.org/10.1186/1471-2105-10-296>.
- [38] R.V. Luckheeram, R. Zhou, A.D. Verma, B. Xia, CD4 + T Cells : differentiation and functions, *Clin. Dev. Immunol.* (2012) 2012, <https://doi.org/10.1155/2012/925135>.
- [39] S.K. Dhanda, S. Gupta, P. Vir, G.P.S. Raghava, Prediction of IL4 inducing peptides, *Clin. Dev. Immunol.* (2013) 1–9, <https://doi.org/10.1155/2013/263952>, 2013.
- [40] G. Nagpal, S.S. Usmani, S.K. Dhanda, H. Kaur, Computer-aided designing of immunosuppressive peptides based on IL-10 inducing potential, *Nat. Publ. Gr.* (2017) 1–10, <https://doi.org/10.1038/srep42851>.
- [41] M.D. Cooper, The early history of B cells, *Nat. Rev. Immunol.* 15 (2015) 191–197, <https://doi.org/10.1038/nri3801>.
- [42] J. Ponomarenko, H.-H. Bui, W. Li, N. Fusseder, P.E. Bourne, A. Sette, B. Peters, ElliPro: a new structure-based tool for the prediction of antibody epitopes, *BMC Bioinf.* 9 (2008) 514, <https://doi.org/10.1186/1471-2105-9-514>.
- [43] H. Bui, J. Sidney, K. Dinh, S. Southwood, M.J. Newman, A. Sette, and vaccines 5 (2006) 1–5, <https://doi.org/10.1186/1471-2105-7-153>.
- [44] A.N. Ilinskaia, M.A. Dobrovolskaia, AC SC, Toxicol. Appl. Pharmacol. (2016), <https://doi.org/10.1016/j.taap.2016.01.005>.
- [45] E. Gasteiger, C. Hoogland, A. Gattiker, S. Duvaud, M.R. Wilkins, R.D. Appel, A. Bairoch, Protein identification and analysis tools on the ExPASy server, in: *Proteomics Protoc. Handb.*, Humana Press, Totowa, NJ, 2005, pp. 571–607, <https://doi.org/10.1385/1-59259-890-0:571>.
- [46] C.N. Magnan, M. Zeller, M.A. Kayala, A. Vigil, A. Randall, P.L. Felgner, P. Baldi, High-throughput prediction of protein antigenicity using protein microarray data, *Bioinformatics* 26 (2010) 2936–2943, <https://doi.org/10.1093/bioinformatics/btq551>.
- [47] A. Roy, A. Kucukural, Y. Zhang, I-TASSER: a unified platform for automated protein structure and function prediction, *Nat. Protoc.* 5 (2010) 725–738, <https://doi.org/10.1038/nprot.2010.5>.
- [48] L. Heo, H. Park, C. Seok, GalaxyRefine : protein structure refinement driven by side-chain, repacking 41 (2013) 384–388, <https://doi.org/10.1093/nar/gkt458>.
- [49] M. Wiederstein, M.J. Sippl, ProSA-web: interactive web service for the recognition of errors in three-dimensional structures of proteins, *Nucleic Acids Res.* 35 (2007), <https://doi.org/10.1093/nar/gkm290>, W407–W410.
- [50] S.C. Lovell, I.W. Davis, W.B.A. Iii, P.I.W. De Bakker, J.M. Word, M.G. Prisant, J. S. Richardson, D.C. Richardson, Structure validation by C _ Geometry : □, □ and C, *Deviation* 450 (2003) 437–450.
- [51] M. Hayes, M. Salvato, Arenavirus Evasion of Host Anti-viral Responses, 2012, pp. 2182–2196, <https://doi.org/10.3390/v4102182>.
- [52] C.D. Cuevas, S.R. Ross, Toll-like receptor 2-mediated innate immune responses against junin virus in mice lead to antiviral adaptive immune responses, *J. Virol.* 88 (2014) 7703–7714, <https://doi.org/10.1128/JVI.00050-14>.
- [53] H.M. Berman, W.F. Bluhm, E. Philip, J. Marvin, H. Weissig, D. John, Research Papers the Protein Data Bank Research Papers, 2002, pp. 899–907.
- [54] D. Kozakov, D.R. Hall, B. Xia, K.A. Porter, D. Padhorny, C. Yueh, D. Beglov, S. Vajda, The ClusPro web server for protein – protein docking 12 (2017) 255–278, <https://doi.org/10.1038/nprot.2016.169>.
- [55] A. Grote, K. Hiller, M. Scheer, R. Münch, B. Nörtemann, D.C. Hempel, D. Jahn, JCat: a novel tool to adapt codon usage of a target gene to its potential expression host, *Nucleic Acids Res.* 33 (2005) W526–W531, <https://doi.org/10.1093/nar/gki376>.
- [56] P.M. Sharp, W. Li, Potential applications, *Nucleic Acids Res.* 15 (1987) 1281–1295.

- [57] N. Rapin, O. Lund, M. Bernaschi, F. Castiglione, Computational immunology meets bioinformatics: the use of prediction tools for molecular binding in the simulation of the immune system, *PLoS One* 5 (2010), e9862, <https://doi.org/10.1371/journal.pone.0009862>.
- [58] E. Krieger, T. Darden, S.B. Nabuurs, A. Finkelstein, G. Vriend, Making optimal use of empirical energy functions: force-field parameterization in crystal space, *Proteins Struct. Funct. Bioinforma.* 57 (2004) 678–683, <https://doi.org/10.1002/prot.20251>.
- [59] C.J. Dickson, B.D. Madej, Å.A. Skjevik, R.M. Betz, K. Teigen, I.R. Gould, R. C. Walker, Lipid14: the amber lipid force field, *J. Chem. Theor. Comput.* 10 (2014) 865–879, <https://doi.org/10.1021/ct4010307>.
- [60] J.R. López-Blanco, J.I. Aliaga, E.S. Quintana-Ortí, P. Chacón, IMODS: internal coordinates normal mode analysis server, *Nucleic Acids Res.* (2014), <https://doi.org/10.1093/nar/gku339>.
- [61] N. Khatoon, R.K. Pandey, V.K. Prajapati, Exploring Leishmania secretory proteins to design B and T cell multi-epitope subunit vaccine using immunoinformatics approach, *Sci. Rep.* (2017) 1–12, <https://doi.org/10.1038/s41598-017-08842-w>.
- [62] D.B. Craig, A.A. Dombkowski, *Disulfide by Design 2 . 0 : a Web-Based Tool for Disulfide Engineering in Proteins*, Disulfide by Design 2 . 0 : a Web-Based Tool for Disulfide Engineering in Proteins, 2013, 0–6.
- [63] N. Nezafat, Z. Karimi, M. Eslami, M. Mohkam, Designing an efficient multi-epitope peptide vaccine against *Vibrio cholerae* via combined immunoinformatics and protein interaction based approaches, *Comput. Biol. Chem.* 62 (2016) 82–95, <https://doi.org/10.1016/j.combiolchem.2016.04.006>.
- [64] U.K. Adhikari, M. Tayebi, M.M. Rahman, Immunoinformatics approach for epitope-based peptide vaccine design and active site prediction against polyprotein of emerging oropouche virus, *J. Immunol. Res.* (2018) 1–22, <https://doi.org/10.1155/2018/6718083>, 2018.
- [65] K.L. Seib, X. Zhao, R. Rappuoli, *Developing Vaccines in the Era of Genomics : a Decade of Reverse Vaccinology*, 2012.
- [66] C.N. Magnan, A. Randall, P. Baldi, SOLpro: accurate sequence-based prediction of protein solubility, *Bioinformatics* 25 (2009) 2200–2207, <https://doi.org/10.1093/bioinformatics/btp386>.
- [67] V. Macromolecular, A. Wlodawer, Chapter 24, 1607 (n.d.) 595–610. <https://doi.org/10.1007/978-1-4939-7000-1>.
- [68] M. Black, A. Trent, M. Tirrell, C. Olive, Advances in the design and delivery of peptide subunit vaccines with a focus on Toll-like receptor agonists, *Expert Rev. Vaccines* 9 (2010) 157–173, <https://doi.org/10.1586/erv.09.160>.
- [69] R.K. Pandey, T.K. Bhatt, V.K. Prajapati, Novel immunoinformatics approaches to design multi-epitope subunit vaccine for malaria by investigating Anopheles salivary protein, *Sci. Rep.* (2018) 1–11, <https://doi.org/10.1038/s41598-018-19456-1>.
- [70] N. Hajighahramani, N. Nezafat, M. Eslami, M. Negahdaripour, S.S. Rahmatabadi, Y. Ghasemi, PT SC department of medical Biotechnology , school of advanced medical sciences and, *Infect. Genet. Evol.* (2016), <https://doi.org/10.1016/j.meegid.2016.12.010>.
- [71] A.J. Shepherd, G. Lee, iBCe-eL : a new ensemble learning framework for improved linear B-cell epitope prediction, *Front. Immunol.* 9 (2018), <https://doi.org/10.3389/fimmu.2018.01695>.
- [72] I. Andersson, H. Karlberg, M. Mousavi-Jazi, L. Martínez-Sobrido, F. Weber, A. Mirazimi, Crimean-Congo hemorrhagic fever virus delays activation of the innate immune response, *J. Med. Virol.* (2008), <https://doi.org/10.1002/jmv.21222>.